DOI 10.34658/9788366741102.10

# Simulation of photon emission by an excited atom in the quantum register

**Marcin Ostrowski**[0000−0001−8985−8123]

*Lodz University of Technology*
*Institute of Information Technology*
*Wólczańska 215, 90-924 Łódź, Poland*
*marcin.ostrowski@p.lodz.pl*

**Abstract.** *This paper investigates whether a quantum computer can efficiently simulate the atom deexcitation process with emission of photon. An algorithm is presented for simulating of the atom-photon interaction and photon free propagation, implemented on standard two-input gates. The paper examines the properties of the proposed algorithm and then compares the obtained results with the theoretical predictions.*
**Keywords:** *quantum computing, quantum simulations, excited state decay*

## 1. Introduction

In the near future, quantum calculations can make a major contribution to the development of informatics [1]. Although practical implementations of quantum computer have not been built yet, its existence seems to be possible. Therefore, it is worth examining the properties of such machines.

Today we know Shor [2] and Grover [3] algorithms which are of lower computational complexity than their best classical counterparts. Another promising application of quantum computer are quantum simulations [4, 5, 6], i.e. the computer modeling of behavior of physical quantum systems. It gives the possibility of effective modeling quantum processes, which is not possible using classical computers [7]. Quantum computers can simulate a wide variety of quantum systems, including fermionic lattice models [8, 9], quantum chemistry [10, 11], and quantum field theories [12].

As is well known, simulations of quantum systems performed using conventional computers are not effective. This means that for classical computer the memory resources and time required to simulate grow exponentially with the size of quantum system. In the case of a quantum computer, the situation is different. The relationship between the size of quantum computer (register) and the size of the

simulated quantum system is linear. Therefore, a very important task is to find the appropriate algorithms that can properly simulate complex quantum systems and non-trivial interactions between them. This is a difficult issue, because most of the interesting quantum systems is feasible in infinitely-dimensional Hilbert spaces. In such situations, we can use the technique of sampling the wave function and build an algorithm based on Quantum Fourier Transform. This case was tested in [13, 14, 15, 16], which examined the free particle and the harmonic oscillator. The main limitation of this coding method of the particle state is that it does not enable implementing an arbitrary potential $V(x)$. It allows only a few special cases such as the $V(x) \sim x^2$ potential. In our previous works we have shown that also rectangular potentials (like thresholds and wells) can be simulated using this method. This provides the ability to examine other interesting processes, such as the tunnel effect [17] and scattering of Pauli[18] and Dirac[19] particle.

Another important issue is the simulation of quantum fields, which are the systems with an infinite number of freedom degrees. In this case, we can replace a continuous band of energy levels with its discrete counterpart. We use this method in the current publication and in [20, 21]. In the above-mentioned works, we have simulated the atom deexcitation process successfully. However, the disadvantage of the used algorithm is sparse coding of states in the quantum register (one level per qubit). For this reason, we could simulate only a few photon energy levels. In this work, we propose a new and more complex algorithm, which enables dense coding of the photon states in the register. In $n_q$ qubits we can encode $2^{n_q}$ photon levels. It allows us to simulate a photon having hundreds energy levels. Therefore, the accuracy of the deexcitation process simulation increase. Moreover, we can now simulate the process of the emitted photon propagation. The algorithm, which is presented here, enables an efficient simulation of more complex processes (e.g. photon emission in many space dimensions or multi-channel decays).

The theoretical approach to the problem of unstable quantum systems decay can be found in [22]. Works of other authors also focus on the simulation of excited states decay. Models based on cavity QED are particularly tested. For example, processes such as: beta decay of helium atom [23] and decay of two-level atom in crystal [24] are examined. In contrast to the cited works, we examine the problem on purely algorithmic grounds, using abstract model of quantum gates. We abstract from specified physical implementation completely.

In order to simulate a quantum register, we used a simple environment written in C++ language for a single processor. However, there is possibility of using parallel computation methods for the simulation of a quantum computer [25]. Moreover, some quantum algorithms can also be studied using neural networks and machine learning models [26].

## 2. Description of the simulated system

Let us consider a complex quantum system which is composed of two parts A and F (Fig. 1). Subsystem A (atom) has two energy levels: level $|0\rangle_A$ with energy equal to zero (the ground state) and level $|1\rangle_A$ with energy $E_A$ (the excited state). We identify subsystem F with photon (without spin) trapped inside one-dimensional cavity of length $x_{max}$ (with periodic boundary conditions ($\psi(0) = \psi(x_{max})$). Base states of subsystem F are denoted by $|n\rangle_F$. We identify state $|0\rangle_F$ with vacuum state (no photon in the cavity). Other states (for $n \neq 0$) are stationary states with wavenumber $k_n$ (given by Eq. (25)) and energy $E_n$ (given by Eq. (26)). In general, parameter $n$ takes both positive and negative values (to simulate the motion of a photon in both directions). Thus, energy spectrum of the photon is two-fold degenerated and (due to the conditions imposed by the simulation) bounded ($|n| \leq n_{max}$).

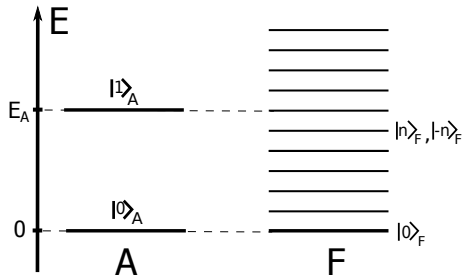


Figure 1. Energy levels of A and F subsystems (in the absence of interactions). All levels of subsystem F except ground state are two-fold degenerated.

The following operator is chosen as the Hamiltonian of interaction between subsystems A and F:

$$\hat{H}_{int} = \sum_{\substack{n=-n_{max} \\ n\neq 0}}^{n_{max}} (g_n \hat{a}^\dagger \hat{b}_n + g_n^* \hat{a} \hat{b}_n^\dagger), \tag{1}$$

where $\hat{a}$ is an operator decreasing energy of subsystem A ($\hat{a}|1\rangle_A = |0\rangle_A$ and $\hat{a}^\dagger|0\rangle_A = |1\rangle_A$) and $\hat{b}_n$ are annihilation operators of subsystem F defined as follows:

$$\hat{b}_n|n\rangle_F = |0\rangle_F \qquad \text{for} \quad 0 < |n| \leq n_{max}, \tag{2}$$

$$\hat{b}_n^\dagger|0\rangle_F = |n\rangle_F \qquad \text{for} \quad 0 < |n| \leq n_{max}. \tag{3}$$

Complex parameters $g_n$ are coupling constants calculated as follows:

$$g_n = -\mathrm{i}\Gamma \sqrt{\frac{E_A}{E_n}} \mathrm{e}^{ik_n x_a}, \tag{4}$$

where $\Gamma$ is decay constant and $x_a$ is position of atom in the cavity. The Hamiltonian (1) describes transitions between states in the following form: $|0\rangle_A|n\rangle_F \leftrightarrow |1\rangle_A|0\rangle_F$. The calculation of $g_n$ and the justyfication of the Hamiltonian (1) is given in Appendix B.
The total Hamiltonian of the system AF has the form:

$$\hat{H} = E_A\hat{a}^\dagger\hat{a} + \sum_{\substack{n=-n_{max}\\ n\neq 0}}^{n_{max}} E_n\hat{b}_n^\dagger\hat{b}_n + \hat{H}_{int}, \tag{5}$$

where $E_n$ are given by Eq. (26).

# 3. The algorithm simulating propagation of free photon

State of photon is encoded in $n_f$-qubit register. State $|00..0\rangle = |0\rangle$ encodes vacuum state. Other base states ($|n\rangle$ for $n = 1, 2 \ldots 2^{n_f} - 1$) encode photon with defined energy and momentum. Let us consider two possibilities:

- photon with positive momentum only ($k_n > 0$):
  In this case, state $|n\rangle$ encodes photon with momentum equal to

  $$k_n = \Delta k \cdot n \quad \text{for} \quad n = 1, 2 \ldots 2^{n_f} - 1, \tag{6}$$

  where by formula (25) $\Delta k = 2\pi/x_{max}$. In this situation $n_{max} = 2^{n_f} - 1$.

- photon with momentum of any sign:
  In this case, the oldest qubit ($n_f - 1$) encodes sign of photon momentum (state $|0\rangle$ corresponds to $k_n > 0$, while state $|1\rangle$ encodes $k_n < 0$ case). The rest of the qubits encode $|k_n|$. Both register states $|00..0\rangle = |0\rangle$ and $|10..0\rangle = |2^{n_f-1}\rangle$ encode vacuum state (but the latter is not used). Other states of the register ($|n\rangle$) correspond to the following values of the momentum:

  $$k_n = \begin{cases} +\Delta k \cdot n & \text{for} \quad n = 1, 2, \ldots 2^{n_f-1} - 1 \\ -\Delta k(n - 2^{n_f-1}) & \text{for} \quad n = 2^{n_f-1} + 1, \ldots, 2^{n_f} - 1 \end{cases} \tag{7}$$

  In this situation $n_{max} = 2^{n_f-1} - 1$.

The algorithm simulating time evolution of free photon (the second component of the Eq. (5)) is shown in Fig. 2. Gates $U_\phi$ are phase-shift gates, which operate according to the scheme:

$$|0\rangle \to |0\rangle, \qquad |1\rangle \to \exp(-i\phi)|1\rangle, \tag{8}$$

where: $\phi = dE\, dt/\hbar$ and $dE = \mathrm{hc}/x_{max}$ is distance between adjacent energy levels.

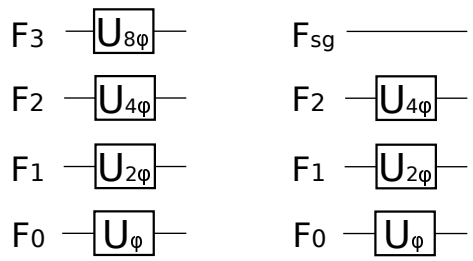


Figure 2. The algorithms simulating free propagation of the photon (example for $n_f = 4$). The left scheme shows the algorithm for $k_n > 0$ only, the right one shows the algorithm for $k_n$ of any sign. The oldest qubit (denoted by $F_{sg}$) encodes sign of $k_n$.

The algorithm from Fig. 2 follows from the fact that diagonal form of time evolution operator is equivalent to phase-shift operator:

$$U_0(dt) = \exp\left(-i\frac{E_n dt}{\hbar}\right) = \exp\left(-i\frac{dE\,dt}{\hbar}n\right) = \prod_{k=0}^{n_L-1} \exp\left(-i\frac{dE\,dt}{\hbar}2^k i_k\right), \qquad (9)$$

where $n_L = 2^{n_f}$. In the last step energy level number $n$ is presented in binary form:

$$n = \sum_{k=0}^{n_L-1} 2^k i_k, \qquad (10)$$

where $i_k$ is $k$-th binary digit of $n$. Therefore, state of $k$-th qubit is multiplied by phase factor $\exp(-i2^k\phi)$ for $i_k = 1$.

# 4. The algorithm simulating interaction between photon and atom

The whole algorithm is shown in Fig. 3. In the first qubit (denoted by A) state of atom is stored. $U_{\phi_A}$ gate is phase shift gate simulating free evolution of subsystem A (first component from Eq. 5). Phase shift angle for $U_{\phi_A}$ gate is equal to $\phi_A = E_A\hbar^{-1}dt$.
Each component of the sum from Hamiltonian (1) (describing transition $|0\rangle_A|n\rangle_F \leftrightarrow |1\rangle_A|0\rangle_F$) is simulated by a separate $R_n$ block. The following transformation is applied:

$$|0\rangle_A|n\rangle_F \rightarrow \cos\phi_{tn}|0\rangle_A|n\rangle_F + ie^{+i\phi_{gn}}\sin\phi_{tn}|1\rangle_A|0\rangle_F, \qquad (11)$$

$$|1\rangle_A|0\rangle_F \rightarrow \cos\phi_{tn}|1\rangle_A|0\rangle_F + ie^{-i\phi_{gn}}\sin\phi_{tn}|0\rangle_A|n\rangle_F, \qquad (12)$$

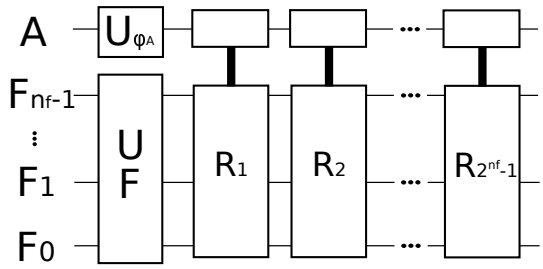


Figure 3. The scheme of the algorithm. UF block implements photon free evolution (Fig. 2). $U_{\phi_A}$ gate simulates free evolution of atom. $R_1, \ldots R_{2^{n_f}-1}$ blocks implement interaction between atom (A) and photon (F). A sample implementation of $R_n$ block is shown in Fig. 4.

where $\phi_{tn} = |g_n|dt/\hbar$, $\phi_{gn} = \mathrm{Arg}(g_n)$ and $g_n$ are given by Eq. (4). Transformations (11)-(12) can be obtained acting on states $|0\rangle_A|n\rangle_F$, $|1\rangle_A|0\rangle_F$ with time evolution operator in the form:

$$U_{int}(dt) = \exp(-i\,dt\,H_{int}/\hbar) = \prod_n \exp\Big(-i\,dt(g_n\hat{a}^\dagger\hat{b}_n + g_n^*\hat{a}\hat{b}_n^\dagger)/\hbar\Big) =$$

$$= \prod_n \sum_{j=0}^{\infty} \frac{1}{j!}\left(-\frac{i\,dt}{\hbar}\right)^j (g_n\hat{a}^\dagger\hat{b}_n + g_n^*\hat{a}\hat{b}_n^\dagger)^j =$$

$$= \prod_n \left(\sum_{j=0}^{\infty} \frac{(-1)^j}{(2j)!}\left(\frac{dt}{\hbar}\right)^{2j} (g_n\hat{a}^\dagger\hat{b}_n + g_n^*\hat{a}\hat{b}_n^\dagger)^{2j} + \right.$$

$$\left. + i\sum_{j=0}^{\infty} \frac{(-1)^j}{(2j+1)!}\left(\frac{dt}{\hbar}\right)^{2j+1} (g_n\hat{a}^\dagger\hat{b}_n + g_n^*\hat{a}\hat{b}_n^\dagger)^{2j+1}\right) \qquad (13)$$

and using the following formulas:

$$(g_n\hat{a}^\dagger\hat{b}_n + g_n^*\hat{a}\hat{b}_n^\dagger)^{2j}|0\rangle_A|n\rangle_F = |g_n|^{2j}|0\rangle_A|n\rangle_F, \qquad (14)$$

$$(g_n\hat{a}^\dagger\hat{b}_n + g_n^*\hat{a}\hat{b}_n^\dagger)^{2j}|1\rangle_A|0\rangle_F = |g_n|^{2j}|1\rangle_A|0\rangle_F, \qquad (15)$$

$$(g_n\hat{a}^\dagger\hat{b}_n + g_n^*\hat{a}\hat{b}_n^\dagger)^{2j+1}|0\rangle_A|n\rangle_F = |g_n|^{2j}g_n|1\rangle_A|0\rangle_F, \qquad (16)$$

$$(g_n\hat{a}^\dagger\hat{b}_n + g_n^*\hat{a}\hat{b}_n^\dagger)^{2j+1}|1\rangle_A|0\rangle_F = |g_n|^{2j}g_n^*|0\rangle_A|n\rangle_F. \qquad (17)$$

Sample implementation of the $R_n$ block (for $n = 5$) is shown in Fig. 4. (For other levels constructing method of $R_n$ blocks is the same.) The first three NOT and CNOT gates implement transformation:

$$|0\rangle_A|n\rangle_F \rightarrow |0\rangle_A|1\ldots1\rangle_F, \qquad (18)$$

$$|1\rangle_A|0\rangle_F \rightarrow |1\rangle_A|1\ldots1\rangle_F. \qquad (19)$$

The last three NOT and CNOT gates implement reverse transformation. Controlled $R_\phi$ gates operate as follows:

$$|0\rangle \to \cos\phi_{tn}|0\rangle + ie^{+i\phi_{gn}} \sin\phi_{tn}|1\rangle, \tag{20}$$

$$|1\rangle \to \cos\phi_{tn}|1\rangle + ie^{-i\phi_{gn}} \sin\phi_{tn}|0\rangle. \tag{21}$$

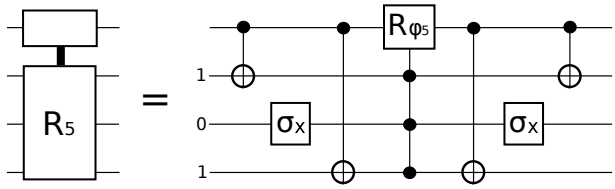


Figure 4. An example of $R_n$ block which simulates an interaction between atom (the highest qubit) with $n = 5$ level of the photon (for $n_f = 3$ and $n_a = 1$). If we write number of level in binary form (in this case: $n = 5 = 101_2$), then we apply $\sigma_x$ gates to each qubit corresponding to 0 binary digits and CNOT gates to each qubit corresponding to 1 binary digits. The least significant bit is at the bottom of the figure.

# 5. The simulation results

## 5.1. Free photon simulation

In the first part of the research, we simulate only photon (system F). In this case an $n_q = 8$ qubit register has been used. The algorithm for photon with momentum of any sign (right scheme in Fig. (2)) has been applied. The other parameters are: $x_{max} = 30\mu$m (cavity length), $dt = 10^{-15}$s (time step of the simulation), $n_1 = 33$ (the number of steps between capturing the state), $\langle x\rangle = 0.5 \cdot 10^{-5}$m (the initial position of packet center in the cavity).
As an initial state of the photon, we choose the Gaussian distribution in the form:

$$\psi_n = \langle\psi|n\rangle = \exp\left(-\frac{(n-\langle n\rangle)^2}{4\,dn} - \mathrm{i}\,k_n\langle x\rangle\right), \tag{22}$$

where $n = 1, 2, \ldots$ is number of energy level in the cavity, $k_n$ is given by Eq. (25). A simple algorithm for inputting state (22) into the quantum register has been proposed in [27].
The results of simulation are shown in Fig. 5. The left plot is made for $\langle n\rangle = 32$ and $dn = 8$, the right one for $\langle n\rangle = 64$ and $dn = 4$.

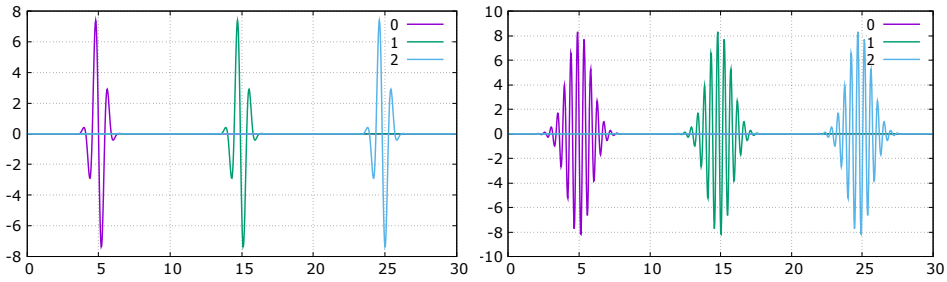


Figure 5. Simulation of free photon propagation. The three phases of motion are shown with interval equal to $3.3 \cdot 10^{-14}$s. The horizontal axis represents position in the cavity (measured in $\mu$m). The vertical axis shows electric field (in kV/m). Transition from momentum to position representation has been made using the formula (27).

## 5.2. The simulation of photon emission by excited atom

In the second part of the research, we simulate the full algorithm from Fig. 3. In this case a $n_q = 9$ qubit register has been used (1 qubit for system A and 8 qubits for system F (with momentum of any sign)). We choose initial state of the system as $|1\rangle_A|0\rangle_F$. Energy of the atom excited level is equal to $E_A = 2$eV. The other parameters are: $x_{max} = 30\mu$m (cavity length), $dt = 10^{-17}$s (time step of the simulation). The results of simulation are shown in Figs 6-10.

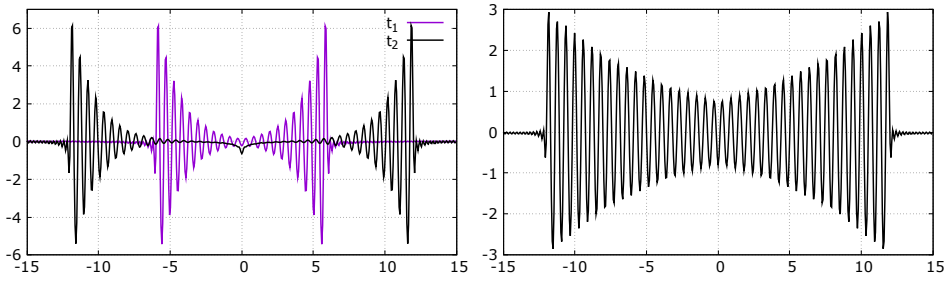


Figure 6. Propagation of the emitted photon in space (for $x_a = 0$). The horizontal axis represents position in the cavity (measured in $\mu$m). The vertical axis shows electric field (in kV/m). The left plot shows case for $\Gamma = 5 \cdot 10^{-21}$J (two phases of motion are shown: for $t_1 = 2 \cdot 10^{-14}$s and $t_2 = 4 \cdot 10^{-14}$s). The right plot is made for $\Gamma = 2 \cdot 10^{-21}$J and $t = 4 \cdot 10^{-14}$s.

In Fig. 7 in addition to the simulation results, we present its approximation (the least squares method) and the theoretical prediction given by formula (e.g.[28]):

$$p_{thr}(t) = \exp\left(-\frac{2\pi}{\hbar}|\tilde{g}|^2 t\right), \tag{23}$$

where $\tilde{g} = \Gamma\sqrt{\frac{d}{dE}}$, $d$ is degeneration of energy levels and $dE = \frac{hc}{x_{max}}$ is distance between adjacent energy levels.

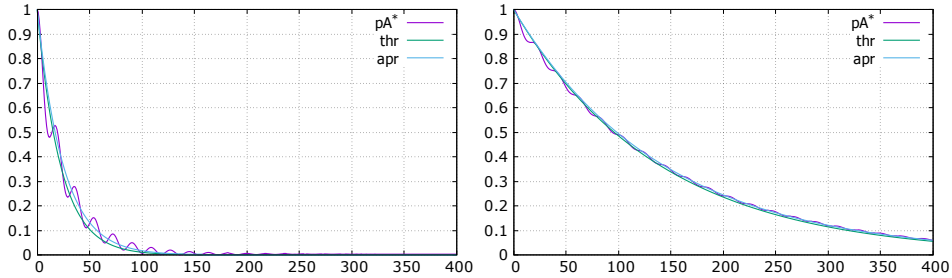


Figure 7. The probability of finding system A in an excited state as a function of time (in $10^{-16}$s units). The left plot is made for $\Gamma = 5 \cdot 10^{-21}$J, the right one for $\Gamma = 2 \cdot 10^{-21}$J. The curves denoted by "thr" are results of theoretical predictions (given by Eq. (23)) and those denoted by "apr" are results of approximation.

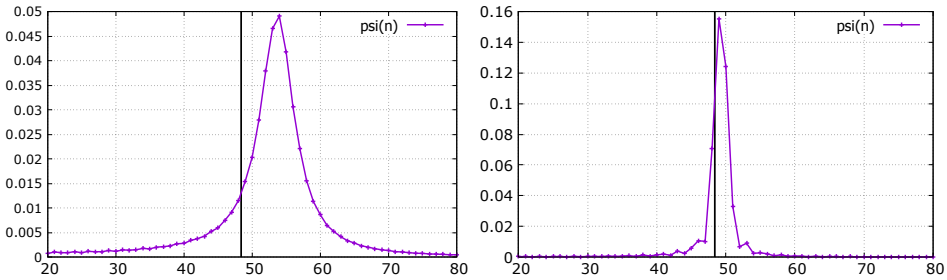


Figure 8. Energy spectrum of the emitted photon. The numbers in the horizontal axis correspond to numbers of energy levels in the cavity ($n$). The left plot is made for $\Gamma = 5 \cdot 10^{-21}$J, the right one for $\Gamma = 2 \cdot 10^{-21}$J. The black vertical line corresponds to the atom excitation energy $E_A = 2$eV (in the absence of atom-photon interaction).

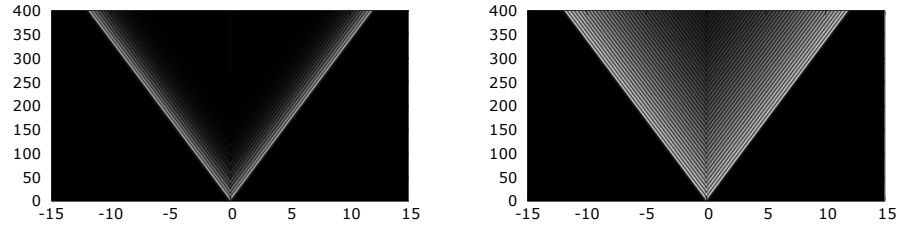


Figure 9. The spacetime diagram for emitted photon. The numbers in the horizontal axis correspond to a position in space (in $\mu$m), whereas the parameters in the vertical axis are equal to time of propagation (in $10^{-16}$s units). The left plot is made for $\Gamma = 5 \cdot 10^{-21}$J and the right one for $\Gamma = 2 \cdot 10^{-21}$J.

In Fig. 10 the propagation of emitted photon is shown in case where the atom is not located in the cavity center ($x_a \neq 0$). We achieve this effect by modification of the phases of $g_n$ coefficients (according to the Eq. (4)).

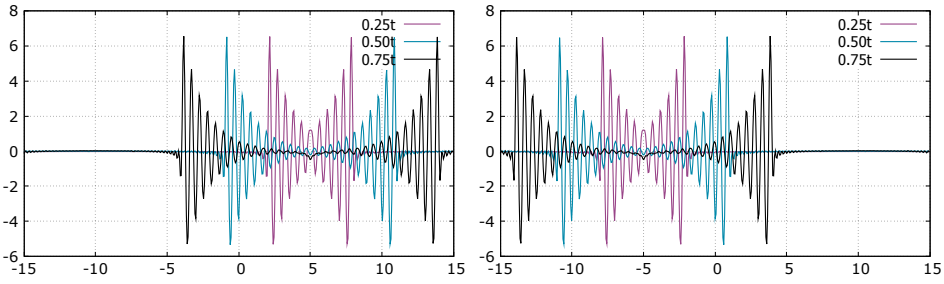


Figure 10. Propagation of the emitted photon in space for changed position of atom inside the cavity. The left plot is made for $x_a = 5\mu$m and the right one for $x_a = -5\mu$m. The vertical axis shows electric field (in kV/m units)). Both plots are made for $\Gamma = 5 \cdot 10^{-21}$J. Three phases of motion are shown with interval equal to $10^{-14}$s.

# 6. Conclusions

- The evidence from this study suggests that even for $n_q = 9$ qubits it is possible to obtain satisfying results. However, the algorithm is scalable - an

increase in the number of qubits means a higher sampling density of photon spectrum and, consequently, more accurate results.

- The results presented in Fig. 7 suggest that the tested algorithm is correct. We obtain good compliance of the results (the curves denoted by "pA*") with theoretical predictions (the curves denoted by "thr").
- The main advantage of the proposed algorithm over its classical counterpart is less memory requirements. The relation between number of simulated energy levels $n_{max}$ and number of qubits is logarithmic, whereas for classical algorithm is linear. For example, a 9-qubit register simulated in this work corresponds to an array of $2 \cdot 2^9 = 1024$ floating point numbers.
- As is well known, a typical lifetime of atom excited states is in the order of $10^{-8}$s (excluding metastable states). This time is much longer in comparison to time of photon propagation in the cavity (the order of $10^{-14}$s). Therefore, the time scale of deexcitation process has been reduced by several orders of magnitude.
- Transition from momentum to position representation given by the formula (27) is made outside the quantum register.

# 7. Appendix A. Useful equations

Let us consider photon in the one-dimensional cavity of length $x_{max}$ with periodic boundary conditions ($\psi(0) = \psi(x_{max})$). Wavelengths of stationary states are given by:

$$\lambda_n = \frac{x_{max}}{n} \quad \text{for} \quad n = 1, 2, \ldots. \tag{24}$$

Photon momentum and wavenumbers are equal to:

$$p_n = \frac{h}{x_{max}} n, \quad k_n = \frac{2\pi n}{x_{max}} \quad \text{for} \quad n = \pm 1, \pm 2, \ldots \tag{25}$$

Energies of the stationary states are given by:

$$E_n = \frac{hc}{x_{max}} |n| = \hbar c |k_n|, \quad \text{for} \quad n = \pm 1, \pm 2, \ldots \tag{26}$$

Electric field $\vec{E}$ related with photon is equal to:

$$E(x,t) = -\sqrt{\frac{\hbar}{\epsilon_0 V}} \sum_n \sqrt{2\omega_n} (\mathrm{im}\{\psi_n(t)\} \cos k_n x + \mathrm{re}\{\psi_n(t)\} \sin k_n x), \tag{27}$$

where $V$ is volume of the cavity.

# 8. Appendix B. Calculation of the $g_n$ coefficients

The total Hamiltonian of electron in atom and electromagnetic field takes the form:

$$\hat{H} = \frac{\vec{p}^2}{2m_e} + V(x) + e\phi, \tag{28}$$

where $m_e$ is electron mass, $V(x)$ is potential energy of electron in atom, $\phi$ is scalar potential of (external) electromagnetic field. Inserting momentum operator $\vec{p} = i\hbar\vec{\nabla} - e\vec{A}$ and omitting the component with $\vec{A}^2$, we obtain (in Coulomb gauge: $\vec{\nabla} \circ \vec{A} = 0$ and $\phi = c \cdot A_0 = 0$) the Hamiltonian of interaction between electron and field in the form:

$$\hat{H}_{int} = -\frac{ie\hbar}{2m_e}\vec{A} \circ \vec{\nabla}, \tag{29}$$

where $\vec{A}$ is vector potential in the form:

$$\vec{A}(x,t) = \sqrt{\frac{\hbar}{\epsilon_0 V}} \sum_{n,s} \frac{1}{\sqrt{2\omega_n}} \left( \vec{\epsilon}_s^{\,*} \hat{b}^\dagger_{n,s} e^{-i(k_n x - \omega_n t)} + \vec{\epsilon}_s \hat{b}_{n,s} e^{i(k_n x - \omega_n t)} \right), \tag{30}$$

$\hat{b}_{n,s}$, $\hat{b}^\dagger_{n,s}$ are the annihilation and creation operators, respectively, and $\vec{\epsilon}_s$ is photon polarization.
The initial and the final state of the system can be expressed as follows:

$$|\psi_i, m_i\rangle = \psi_i(\vec{r}) \otimes \frac{1}{\sqrt{m_i!}} (\hat{b}^\dagger_{k_n,s})^{m_i} |0\rangle, \tag{31}$$

$$|\ _f, m_f\rangle = \psi_f(\vec{r}) \otimes \frac{1}{\sqrt{m_f!}} (\hat{b}^\dagger_{k_n,s})^{m_f} |0\rangle, \tag{32}$$

where $\psi_i$ and $\psi_f$ are the initial and the final wave function of electron, respectively, $|m_i\rangle$ is the $m_i$-photon initial state (for single mode), whereas $|m_f\rangle$ is the $m_f$-photon final state.
Matrix elements of the interaction Hamiltonian (29) take the form:

$$\begin{aligned} \langle m_i, \psi_i | \hat{H}_{int} | \psi_f, m_f \rangle = \\ = -\frac{ie}{m_e} \sqrt{\frac{\hbar^3}{8\epsilon_0 V \omega_n}} \ \sqrt{m_i}\delta_{m_i, m_f+1} \vec{\epsilon}_s^{\,*} \circ \left( \int d^3\vec{r}\, \psi_i^*(\vec{r}) e^{-i(k_n x - \omega_n t)} \vec{\nabla} \psi_f(\vec{r}) \right) + \\ + \sqrt{m_f}\delta_{m_i+1, m_f} \vec{\epsilon}_s \circ \left( \int d^3\vec{r}\, \psi_i^*(\vec{r}) e^{i(k_n x - \omega_n t)} \vec{\nabla} \psi_f(\vec{r}) \right) \Bigg). \end{aligned} \tag{33}$$

In this work transitions between one-photon states and vacuum state are only considered. Additionally, we assume that the size of atom is much smaller than the

emitted photon wavelength. In this case, the $g_n$ coefficients can be expressed as follows:

$$g_n = \langle 0, \psi_i | \hat{H}_{int} | \psi_f, 1 \rangle = -\frac{ie}{m_e} e^{ik_n x_a} \sqrt{\frac{\hbar^3}{8\epsilon_0 V \omega_n}} \int d^3\vec{r} \psi_i^*(\vec{r}) \vec{\epsilon} \circ \vec{\nabla} \quad _f(\vec{r}), \qquad (34)$$

where $x_a$ is the position of atom in the cavity.

# References


[1] Feynman, R. *Internat. J. Theor. Phys.*, 21:467–488, 1982.

[2] Shor, P. W. *Proc 35th Ann. Symp. Found. Comp. Sci., IEEE Comp.Soc. Pr.*, 124, 1994.

[3] Grover, L. K. From schrodinger equation to the quantum search algorithm. *Am. J. Phys.*, 69:769–777, 2001.

[4] Lloyd, S. Universal quantum simulators. *Science*, 273:5278, 1996.

[5] Schaetz, T., Monroe, C., and Esslinger, T. Focus on quantum simulation. *New Journal of Physics*, 15:085009, 2013.

[6] Lanyon, B. P. Universal digital quantum simulation with tapped ions. 2011.

[7] Childs, A., Maslov, D., Nam, Y., Ross, N., and Su, Y. Toward the first quantum simulation with quantum speedup. *PNAS*, 115(38), 2018.

[8] Wecker, D. Solving strongly correlated electron models on a quantum computer. *Phys Rev A*, 92:062318, 2015.

[9] Kokail, C., Maier, C., and van Bijnen, R. Self-verifying variational quantum simulation of lattice models. *Nature*, 569, 2019.

[10] Wecker, D., Bauer, B., Clark, B., Hastings, M., and Troyer, M. Gate count estimates for performing quantum chemistry on small quantum computers. *Phys Rev A*, 90:022305, 2014.

[11] Hempel, C., Maier, C., and Romero, J. Quantum chemistry calculations on a trapped-ion quantum simulator. *Phys. Rev. X*, 8:031022, 2018.

[12] Jordan, S., Lee, K., and Preskill, J. Quantum algorithms for quantum field theories. *Science*, 336:1130–1133, 2012.

[13] Wiesner, S. Simulation of many-body quantum systems by a quantum computer. 1996.

[14] Zalka, C. Efficient simulation of quantum system by quantum computers. *Fortschr. Phys.*, 46:877–879, 1998.

[15] Strini, G. Error sensitivity of a quantum simulator i: a first example. *Fortschr. Phys.*, 50:171–183, 2002.

[16] Benenti, G. and Strini, G. Quantum simulation of the single-particle schrödinger equation. 2007.

[17] Ostrowski, M. Quantum simulation of the tunnel effect. *Bulletin of the Polish Academy of Sciences Technical Sciences*, 63(2):379–383, 2015.

[18] Ostrowski, M. Quantum simulaton of the pauli particle. *Przeglad Elektrotechniczny, ISSN 0033-2097*, 89(7), 2013.

[19] Ostrowski, M. Quantum simulation of the dirac particle. *Open Systems & Information Dynamics*, 22(1):1550002, 2015.

[20] Ostrowski, M. Simulation of the excited state decay in the quantum register. *Prz. Elektrotechniczny*, (10):167–169, 2020.

[21] Ostrowski, M. Simulation of the schrödinger particle nonelastic scattering with emission of photon in the quantum register. *Bull. Pol. Ac.: Tech.*, 68(5), 2020.

[22] Anastopoulos, C. Decays of unstable quantum systems. *Int J Theor Phys*, 58:890–930, 2019.

[23] Vaintraub, S., Blaum, K., Hass, M., Heber, O., Aviv, O., Rappaport, M., Dhal, A., Mador, I., and Wolf, A. Simulations of $\beta$-decay of $^6$he in an electrostatic ion trap. 2014.

[24] Buzek, V., Drobny, G., Kim, M., Havukainen, M., and Knight, P. Numerical simulations of atomic decay in cavities and material media. *Phys.Rev.A*, 60(1):582–592, 1999.

[25] Sawerwain, M. and Pilecki, J. Parallel implementation of a quantum computing simulator. *Journal of Applied Computer Science*, 14(2), 2006.

[26] Citko, W. and Sienko, W. Realizowalnosc algorytmow kwantowych z zastosowaniem opartych na sieciach neuronowych modeli uczenia maszynowego. *Przeglad Elektrotechniczny*, (9):146, 2019.

[27] Ostrowski, M. Loading initial data into the quantum register. In *XV International Conference "System Modelling and Control", Łódź, Poland, 23-24 September 2013*. 2013.

[28] Haken, H. *Light: Waves, photons, atoms*. North-Holland Pub. Co., 1985.